Surface scanning of anthropological specimens: nominal-actual comparison with low cost laser scanner and high end fringe light projection surface scanning systems

Oberflächenscannen anthropologischer Objekte: Soll-Ist Vergleiche mit einem niedrigpreisigen Laserscanner und hochpreisigen Streifenlicht Scanner Systemen

Astrid Slizewski[1]*, Martin Friess[2] & Patrick Semal[3]

[1] Neanderthal Museum, Talstrasse 300, D-40822 Mettmann
[2] Muséum national d'Histoire naturelle & UMR7206 du CNRS, 43, rue Buffon, F-75005 Paris
[3] Royal Belgian Institute of Natural Sciences, 29 rue Vautier, B-1000 Bruxelles

Abstract - We tested three surface scanning systems: the low cost NextEngine laser scanner, the white light Fringe Projection Breuckmann Smartscan and the white light Fringe Projection Steinbichler COMET V 4M. We evaluate the potential of such systems for digitalizing original anthropological specimens and compare it with a "nominal" 3D model derived from µCT or CT data. Our results show that surface scanning of teeth is generally problematic even for high end systems. Even though studies of the occlusal surface are possible with high end systems, high resolution µCT still has to be considered the best choice for scientific studies dealing with details of the occlusal surface. However, for general digitalization purposes and recording of dimensions even the NextEngine system is suitable.
In our tests, Breuckmann Smartscan produced the best models with the lowest deviation compared to the nominal µCTmodel. The Steinbichler is the fastest system but the quality of the resulting models is slightly lower. NextEngine produces a clearly lower quality than the tested high end systems but if one considers the different price margins of the systems, the proportionally good data provided by NextEngine is remarkable. In the case of bones with a simple geometric structure, this low cost scanner can compete easily with 3D models derived from medical CT for gross morphometric studies.

Zusammenfassung - *In diesem Artikel werden drei Oberflächenscanner getestet: der preisgünstige NextEngine Laser, der Weißlichtstreifenscanner Breuckmann SmartScan und der Weißlichtstreifenscanner Steinbichler COMET 4M. Das Potential der unterschiedlichen Modelle für die Digitalisierung anthropologischer Objekte wird durch den Vergleich zu einem "Soll"-Modell auf Basis von CT-Scans betrachtet. Die Ergebnisse zeigen, dass das Scannen von Zähnen selbst für absolut hochwertige Systeme problematisch ist. Obwohl morphologische Studien der Kauflächen anhand von Oberflächenscans hochwertiger Systeme prinzipiell möglich sind, bleiben CT Daten für wissenschaftliche Studien weiterhin die erste Wahl. Für einfach Digitalisierungsvorgänge ist der NextEngine Laser Scanner jedoch zu empfehlen.*
Bei unseren Tests zeigte der Breuckmann SmartScan die besten Ergebnisse mit der geringsten Abweichung zu den Soll-Modellen. Das Steinbichler System war das schnellste, die Qualität der Ergebnisse ist minimal schlechter. Das NextEngine System produziert deutlich schlechtere Ergebnisse als die hochwertigen Systeme, in Anbetracht des niedrigen Preislevels sind die Ergebnisse jedoch von erstaunlich guter Qualität. Bei Knochen mit einfacher geometrischer Struktur können die Scan Ergebnisse des NextEngine mit den 3D-Daten hochwertiger Systeme mithalten.

Keywords - 3d scanner; virtual anthropoplogy; digitalization; tooth; bone; enamel; laser; white light Fringe Projection
3D Scanner; Virtuelle Anthropologie; Digitalisierung; Zahn; Knochen; Zahnschmelz, Laser; Streifenlichtprojektion

Introduction

The increasing importance of computer applications in archaeology and paleoanthropology has been stated by many authors (e.g. Borderie et al. 2004; Gibbons 2002; Guipert et al. 2003; Mafart & Delignette 2002; Mafart et al. 2004; Recheis et al. 1999; Sumner & Riddle 2008; Weber et al. 1998; Weniger et al. 2007). This requires the digitalization of the investigated objects. In a previous paper, we described the technology of surface scanning systems and presented the results of tests on different materials of interest (flint, ceramics, bone) with

*corresponding author:
slizewski@neanderthal.de

different scanner types ranging from low cost to high end models (Slizewski & Semal 2009).

Recently, the low priced surface scanning system NextEngine was used successfully in paleoanthropological investigations (see e.g. Benazzi et al. 2009; DeSilva 2009; Tocheri et al. 2007). Our own studies have also shown that the surface texture of bones is unproblematic for the NextEngine scanner and that it can produce good results if the geometry of the anatomical element is not too complex (Slizewski & Semal 2009). This is the case in the cited studies dealing with a clavicle (Benazzi et al. 2009) and a phalanx (DeSilva 2009).

In this study, the question of interest was whether the NextEngine also allows small complex objects, such as teeth, to be digitalized in a quality suitable for scientific purposes. If so, the low price (about €3 000) of this laser scanning system could open the possibility of extensive collection digitalization for many anthropological institutions, otherwise unable to afford the standard prices of high end scanner (from €60 000 upwards). Database projects (e.g. Kullmer et al. 2002; Weniger et al. 2007) could greatly benefit from this.

Material

Neanderthal Material

We scanned the teeth NN31 and NN33 found in 1997 at the site of the former Feldhofer Cave (Neandertal) in the valley of the River Düssel near Mettmann (Germany). NN31 is a right upper M2 which exhibits mesially a 6.8 mm long interproximal ‚tooth pick' groove. NN33 is a left upper M3 of a Neandertal that is missing the lingual root. An anthropological description was published by Fred Smith (in Schmitz et al. 2003).

Spy Material

For comparison with other small sized bones, we also used the proximal phalanx Spy 425 which is symmetrical to Spy 25G belonging to the original collection discovered by M. Lohest and M. de Puydt in 1886 (Fraipoint & Lohest 1887). Spy 425 was discovered in the Spy fauna remains collection by I. Crevecoeur and H. Rougier in the framework of a new study of the collection (Rougier et al. 2004). It was directly dated to the Neolithic, showing that anatomically modern human bones were mixed in with the Neanderthal specimens in the original collection (Semal et al. 2009). The last specimen is the Neanderthal talus Spy 18 from the original Spy collection.

Digitalization

µCT and CT

CT scans of NN31 and NN33 were done by a computed tomography scanner with a capability of 225 kV (300 W) and a voxel size of 44µ. Both teeth were scanned in one part with 1440 projections / 360°.

Spy 425 was µscanned by the µComputed Tomography unit of the University of Antwerp with a Skyscan 1076 invivo µCT with 17.68 µm pixel size resolution. The bone was scanned in three parts and no specific alignment post-treatment was used. This explains a slight discrepancy between the three parts. The Spy 18 talus was scanned during the TNT project with the last generation of medical CT (Siemens Sensation 64) with a pixel size of 191 µm and a slice thickness of 0.6 / 0.3 mm (Semal et al. 2005). Surface models were obtained with Avizo 6.1. Segmentation was performed in order to remove all the internal structures and keep just the external surface of the specimen.

Specifications of CT scans and stl reconstruction are listed in Figure 1. STL (Surface Tesselation Language) is a very common format for 3D data.

NextEngine

Newer versions of the NextEngine application have been launched since our first study. At the beginning

	Steinbichler Comet V	Breuckmann SmartScan 3D	NextEngine
Price	c. €110 000 - €120 000	c. €60 000 - €90 000	c. €1 990 - €2 650
Automatic turntable	yes	yes	yes
Camera resolution	2048 x 2048	1384 x 1036	3 Megapixel
Accuracy	5µm	9µm	125µm
Operating system	64bit	32 bit (64bit optional)	64bit
Software included	COMETplus	OPTOCAT	Scanstudio HD Pro
Data interface	IGES, VDA, STEP, STL, Pro/E, Catia V4, Catia V5, PLY, ACIS, ASCII	ASCII, BRE, STL, PLY, VRML	VRML, STL, U3D, PLY, XYZ, OBJ
Texture	no	yes	yes

Fig. 1. Specifications of surface scans.

Abb. 1. *Spezifikationen der Oberflächenscans.*

	CT NN31	CT NN33	CT Spy18	CT Spy425
Capability	225kV	225kV	120kV	100 kV
Voxel size	44 µm	44 µm	191,4 µm	17,68 µm
Number of projections	1440/360°	1440/360°	---	360/180°
Scans done	1	1	1	3
Slice thickness	45 µm	45 µm	0,6/0,3 mm	17.68 µm
Convolution filter	1.00	1.00	H60s	Beam Hardening 61 %
ROI	409.60 mm	409.60 mm	98.00 mm	No
Threshold value	340	340	54	32

Fig. 2. Specifications of CT scans.
Abb. 2. *Spezifikationen der CT Scans.*

of 2009, NextEngine released a new Scanstudio HD Pro allowing an increase of the point density to 160 000 points by square inch or halving the acquisition time for lower resolutions. The scans produced with this new version of the software permit more detailed 3D models. Nevertheless, the 32 bit application drastically limited the possibility of effectively using this High Definition mode on a complete 3D model. In November 2009, NextEngine released a 64 bit version of the Scanstudio HD application and it is now possible to use more than 4 GB of RAM. This allows a complete 360° rotation with HD settings. The version improves also the alignment and the fusion of models.

Acquisition of samples: We produced two sets of 360° acquisition from 16 angles in medium mode at the highest resolution (40 000 points by square inch) with neutral light settings. Scanstudio HD pro was used for the alignment, the fusion and the filling of holes.

Steinbichler COMET V

The Steinbichler COMET V is available with a camera up to 11 Megapixel. We used a version with a 4 Megapixel camera. The COMET V works with a one-camera-technique and white light Fringe Projection.

Acquisition of samples: We used a measuring field of 100x100x100 mm to scan the tooth NN33. For a complete model of the tooth we did two sets of 360° acquisition from eight angles. The 360° acquisition was done with exposure fusion (180ms and 360ms). In addition, we did two single shots with exposure fusion (90ms, 180ms and 360ms). Models were aligned with COMETplus software.

Breuckmann Smartscan 3D

The Breuckmann Smartscan Duo system is based on a combination of Moiré-topography, phase shift and grey code techniques. It uses two 1.4 Mpixel RGB cameras and a fringe pattern projector to capture both geometry and texture. For a measurement field of 90mm, the nominal resolution is 55µm, with a manufacturer-specified measurement precision of 9µm. Acquisitions were taken along a 360° arc at variable angles, alignment and merging was performed with Breuckmann's proprietary software (Optocat).

Acquisition of samples: Using Geomagic studio, the stl models were aligned to a common orientation and registered using least-squares algorithms. Three descriptive statistics are derived from this registration, which are the maximum and average difference, and the standard deviation.

Specifications of the surface scanner are listed in Figure 2.

Methods

Once the scans were completed, we generated nominal-actual models, using the µCT-derived STL model set as the nominal model with which all models from surface scanner are compared. The nominal-actual models show the deviation of the surface scans from the CT data.

By defining the µCT-model as the reference, or „true" model, the average deviation computed for each surface model reflects the accuracy of the surface scanner, while the standard deviation expresses the precision (reliability) of that measurement. We do not presume µCT-data to be error-free, but we choose this solution in order to generate objective comparisons of the different surface scanner. The nominal-actual models were created with the software packages INSPECT plus and Geomagic 11.

Results

NN31

NextEngine and Breuckmann Smartscan 3D scanner are able to capture texture (Fig. 3). This is of secondary interest if just surface is needed but it could be useful in order to see small details, such as small enamel fractures or structures like sub-vertical grooves or tooth pick grooves not acquired by the surface scanning but visible on the texture model. The µCT derived model allows these structures to be seen precisely. The Breuckmann Smartscan 3D surface model allows recognition of some of the sub-vertical grooves on the surface model, whereas these structures are only visible on the texture model for NextEngine. The Breuckmann Smartscan 3D model

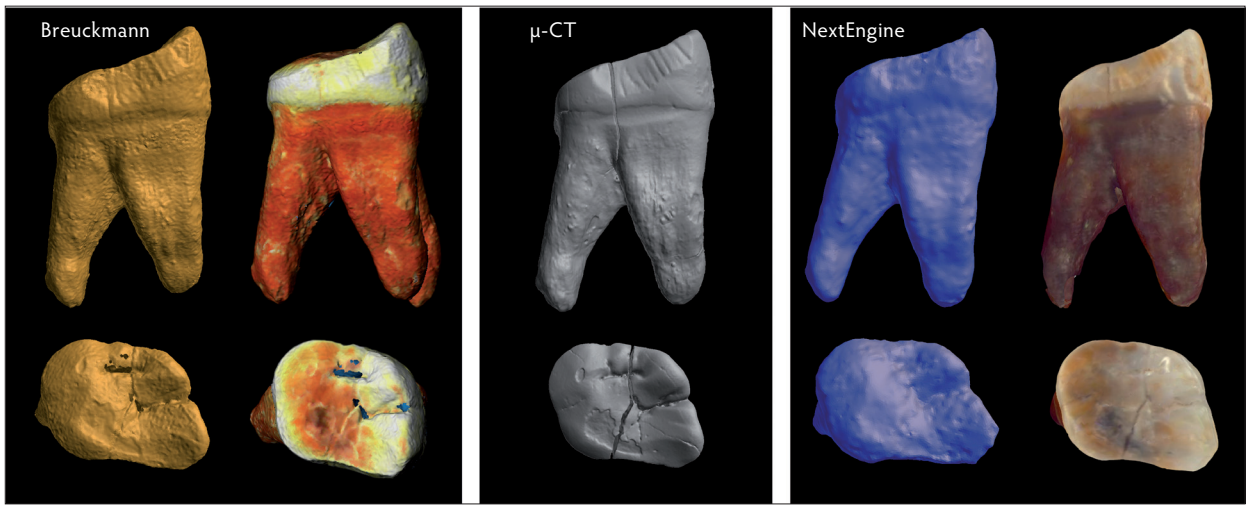

Fig. 3. 3D rendered stl / texture model of NN31. Left : Breuckmann Smartscan 3D structured light surface scanner; Center: µCT derived stl model; Right : NextEngine laser surface scanner.

Abb. 3. *3D generiertes stl / Oberflächenmodel von NN31. Links: Breuckmann smartscan 3D Oberflächenscanner mit strukturiertem Licht; Mitte: STL Model generiert aus µCT Daten; Rechts: NextEngine Laserscanner.*

displays more details while NextEngine is limited to the general morphology of the tooth (Fig. 3). Figure 4 summarizes the results of the nominal-actual models obtained with COMET Inspect and Geomagic softwares. The average deviation of the NextEngine scanner NN31 model is about 50 µm while the maximum deviation is about 300 - 350 µm. The Breuckmann Smartscan 3D model has an average deviation of 23 µm and a maximum deviation ranging between 170 and 340 µm. Figures 5 and 6 display the difference-maps obtained respectively with Inspect plus and Geomagic 11.

NN33

Figure 7 summarizes the results of the nominal-actual models obtained with COMET Inspect and Geomagic softwares. NextEngine model displays an average deviation about 57 µm with a maximum deviation of 419 µm. Nevertheless these maximum error points are located in the missing parts of the acquisition which were estimated during the fusion process and the holes filling (see Fig. 8). The Breuckmann Smartscan 3D

	COMET INSPECT	Geomagic Studio
CT - NEXTENGINE		
Average deviation	50 µm	52 µm
Maximum deviation	305 µm	344 µm
Standard deviation		50 µm
CT - BREUCKMANN SMARTSCAN		
Average deviation	23 µm	22 µm
Maximum deviation	169 µm	343 µm
Standard deviation		30 µm

Fig. 4. Nominal-actual models of NN31 obtained with the COMET Inspect and Geomagic softwares.

Abb. 4. *Soll-Ist Modelle von NN31, erzeugt mit den Programmen COMET Inspect und Geomagic.*

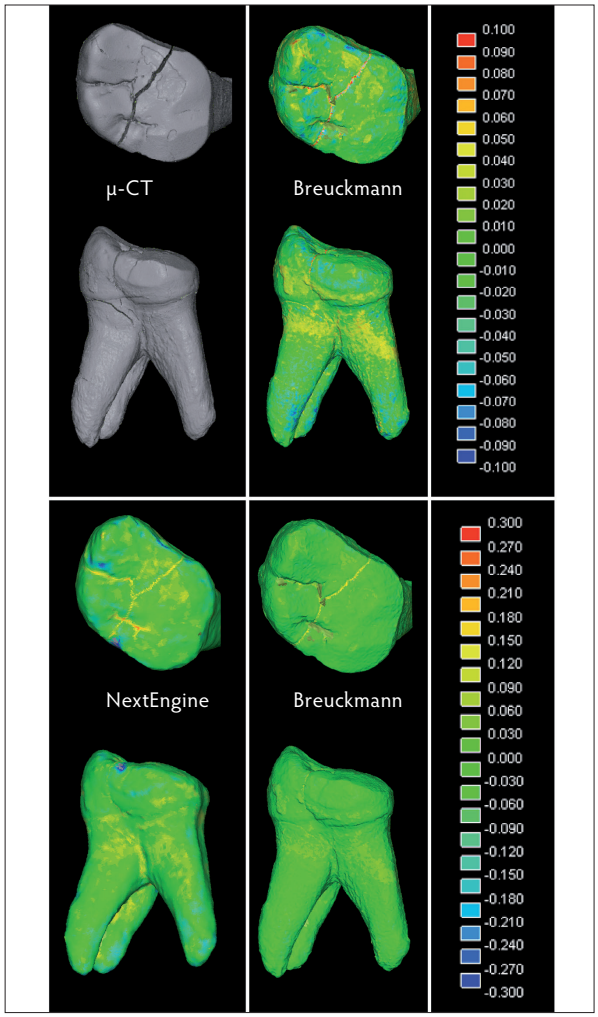

Fig. 5. Difference-map of µCT/Surface scannners Breuckmann Smartscan 3D and NextEngine for NN31. Top : -0,1/0,1mm scale. Bottom : -0,3/0,3 mm scale. Generated by Comet INSPECTplus.

Abb. 5. *Abweichungskartierung vom µCT/Oberflächenscanner Breuckmann Smartscan 3D und NextEngine für NN31. Oben: -0,1/0,1mm Skala. Unten: -0,3/0,3 mm Skala. Erzeugt mit Comet INSPECTplus.*

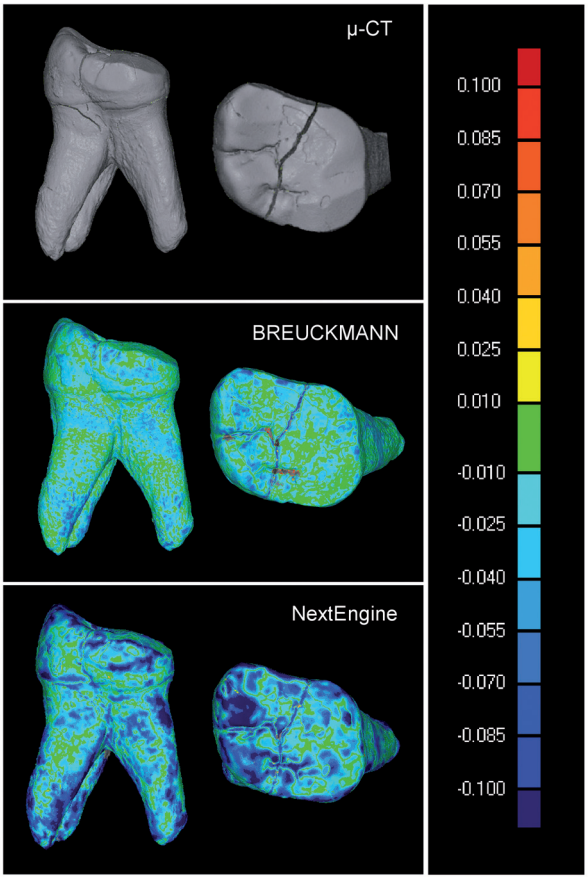

Fig. 6. Difference-map of µ-CT/Surface scannners Breuckmann Smartscan 3D and NextEngine for NN31. Generated by Geomagic 11 with -0,1/0,1mm scale.

Ab. 6. *Abweichungskartierung vom µCT/Oberflächenscanner Breuckmann Smartscan 3D und NextEngine für NN33. Erzeugt mit Geomagic 11 und einer -0,1/0,1mm Skala.*

model has an average deviation of 23 µm with a maximum deviation ranging between 258 - 337 µm. The average deviation of the COMET V model is about 35 µm while the maximum deviation is 126 µm by the COMET Inspect and 337 µm by Geomagic 11.

	COMET Inspect	Geomagic Studio
CT - NEXTENGINE		
Average deviation	57 µm	53 µm
Maximum deviation	419 µm	335 µm
Standard deviation		49 µm
CT - BREUCKMANN SMARTSCAN		
Average deviation	23 µm	22 µm
Maximum deviation	258 µm	337 µm
Standard deviation		34 µm
CT - STEINBICHLER COMET V		
Average deviation	35 µm	29 µm
Maximum deviation	126 µm	337 µm
Standard deviation		40 µm

Fig. 7. Nominal-actual models of NN33 obtained with the COMET Inspect and Geomagic softwares.

Abb. 7. *Soll-Ist Modelle von NN33, erzeugt mit den Programmen COMET Inspect und Geomagic.*

An important deviation is seen in the scissures on the occlusal surface. The irregular, small-sized cavities seem to be captured differently depending on the scanner type. NextEngine provides just the general morphology with a very poor level of details. The Steinbichler stl model displays more details but cannot replace the µCT. The Breuckmann Smartscan 3D stl model fails to display the smallest details of the occlusal surface but the level of detail is considerably higher than that of the two other scanners (Figs. 9 - 11).

Spy 425

We also evaluate NextEngine for the scanning of small bones like hand and foot bones. The NextEngine scanner is already used by different anthropologists (Tocheri et al. 2007). The goal of this study is to compare, as in the case of the teeth, the stl produced by the NextEngine scanner with a "nominal" model obtained from µCT data. We used the proximal phalanx Spy425 which was µ-scanned before radio-carbon analysis sampling.

Figure 12 summarizes the results of the nominal-actual models obtained with COMET Inspect software. As for teeth NN31 and NN33, the average deviation is about 100 µm and the maximum deviation is 350-415 µm. We have to note that part of the error is not derived from the NextEngine scan but from the misalignment of the 3 µCT sub scans of the phalanx (see the oblique lines on the µCT model and on the comparison map). The level of detail is lower than the µCT model but probably enough for many procedures, allowing the use of NextEngine for specific purposes (Fig. 13).

Spy 18

Finally we tested the NextEngine with a talus, which is one of the biggest of the small human bones with a relatively simple morphology. We compared the stl produced by NextEngine with a model derived from medical CT data.

Figure 14 summarizes the results of the nominal-actual models obtained with COMET Inspect software. The average deviation is about 145 µm but the maximum deviation is high with values greater than an half a millimeter.

Figure 15 displays the difference map. Most of the surface is in green colors but some spots display larger differences. The detailed view of figure 16 shows that these differences are related to areas where the cancellous bone is exposed. The very complex structure of the cancellous bone is not correctly recorded by the NextEngine scanner but the general level of details is better on the NextEngine stl model than on the CT stl model (Fig. 15).

Conclusions

The three tested scanners have very different prices from €3 000 to €110 000. The results show clearly that

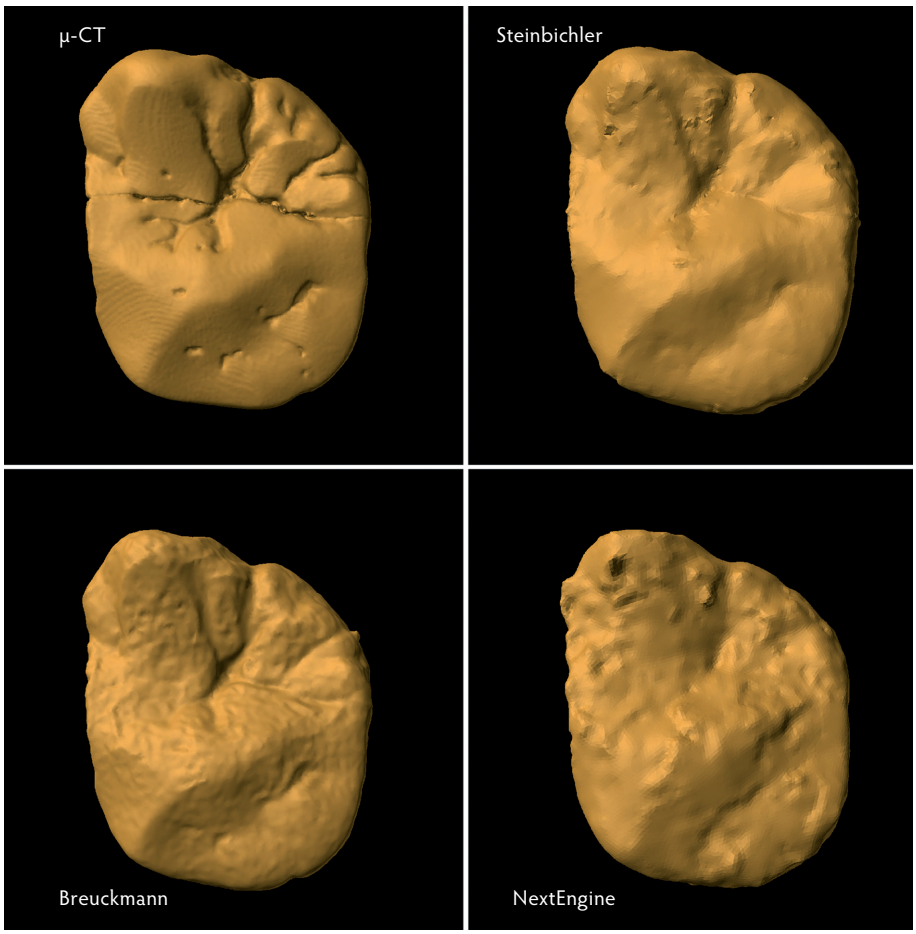

Fig. 8. Occlusal views from stl models produces from µCT, Surface scanners Steinbichler Comet V, Breuckmann Smartscan 3D and NextEngine for NN33. Rendering with Meshlab 1.2.2b (http://www.sourceforge.net).

Abb. 8. *Okklusale Ansichten der STL Modelle erzeugt aus µCT Daten und den Oberflächenscans des Steinbichler Comet V, Breuckmann Smartscan 3D und NextEngine von NN33. Gerendert mit Meshlab 1.2.2b (http://www.sourceforge.net).*

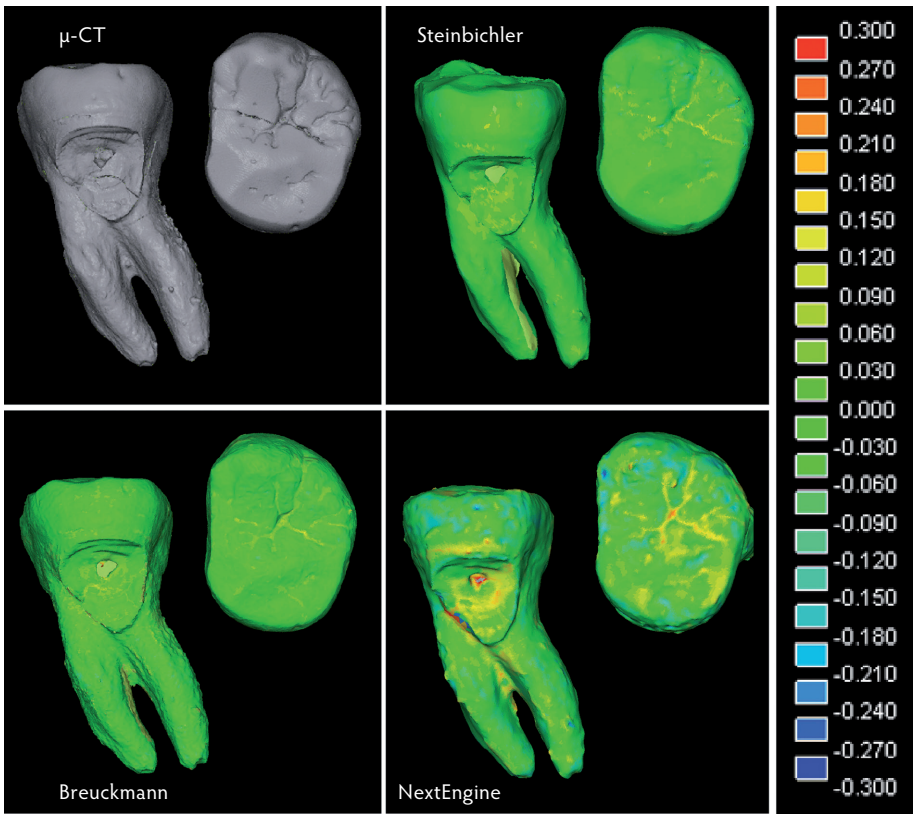

Fig. 9. Difference-map of µ-CT/Surface scanners Steinbichler Comet V, Breuckmann Smartscan 3D and NextEngine for NN33. Generated by Steinbichler INSPECTplus with -0.3/0.3 mm scale.

Abb. 9. *Abweichungskartierung vom µCT/Oberflächenscanner Steinbichler Comet V, Breuckmann Smart-scan 3D und NextEngine für NN33. Erzeugt mit Steinbichler INSPECTplus mit einer -0,3/0,3 mm Skala.*

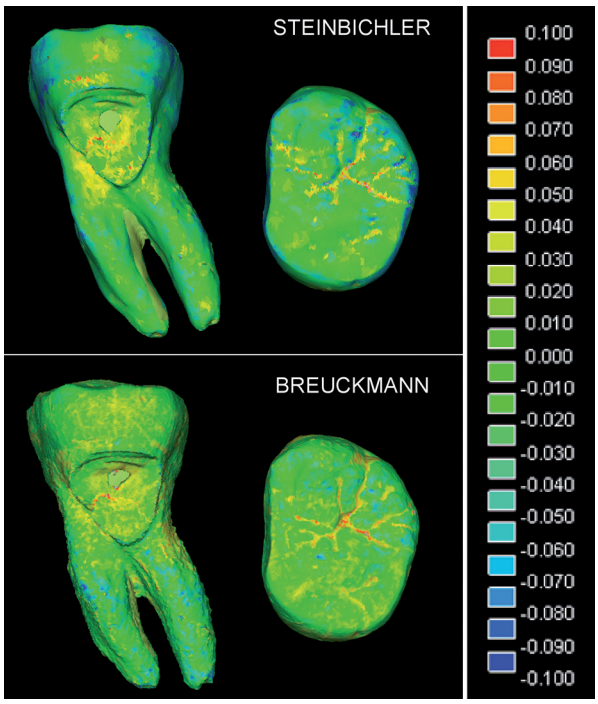

Fig. 10. Difference-map of µ-CT/Surface scanners Steinbichler Comet V and Breuckmann Smartscan 3D for NN33. Alignment and difference with Steinbichler INSPECTplus with -0.1/0.1 mm scale.

Abb. 10. *Abweichungskartierung vom µCT/Oberflächenscanner Steinbichler Comet V, Breuckmann Smartscan 3D und NextEnginefürNN33.ErzeugtmitSteinbichlerINSPECTplusmiteiner -0,1/0,1 mm Skala.*

the surface models produced by high end scanners have a better resolution and a higher level of details. The average deviation ranges between 22 µm for the Breuckmann Smartscan 3D scanner to 50 µm for the NextEngine one. Nevertheless the 50 µm average

	COMET Inspect
CT - NEXTENGINE	
Average deviation	95 µm
Maximum deviation	368 µm

Fig. 12. Nominal-actual model of Spy425 obtained with COMET Inspect

Abb. 12. *Soll-Ist Modell von Spy425, erzeugt mit dem Programm COMET Inspect*

difference is still excellent, considering the price of about €3 000. However, surface scanners are still not really able to replace µCT scans if the purpose is scientific micromorphological research on teeth or high resolution digital backup (see Fig. 8). Details of the occlusal surface such as scissures and protuberances, which are important in studies concentrating on e.g. phylogenetic (e.g. Singleton 2003) or nutrional (e.g. Ulhaas et al. 2007) aspects, are not captured precisely enough by the NextEngine or the COMET V scanner. The Breuckmann Smartscan provides better details on the stl model than the two other systems but it is at the limit for certain aspects of palaeoanthropological research. Capturing the different textures of tooth root and crown is challenging for technology based upon the reflection of light. This problem can be solved by making different sets of scans with different light settings. However, even in a mode that allows the highest data capturing, the enamel of the crown still reflects too much light and the laser or white light fringe ingresses too deep into the surface to produce data which can generate details accurately enough for scientific research. Further improvements of the technology have to be made in order to obtain better scanning of enamel. The scan of replicas is another alternative

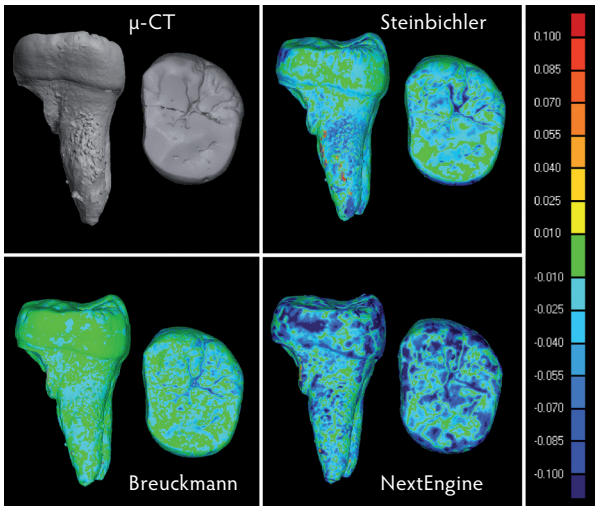

Fig. 11. Difference-map of µ-CT | Surface scanners Steinbichler Comet V, Breuckmann Smartscan 3D and NextEngine for NN33. Generated by Geomagic 11 with -0.1/0.1 mm scale.

Abb. 11. *Abweichungskartierung vom µCT | Oberflächenscanner Steinbichler Comet V, Breuckmann Smartscan 3D und NextEngine für NN33. Erzeugt mit Geomagic 11mit einer -0,1/0,1 mm Skala.*

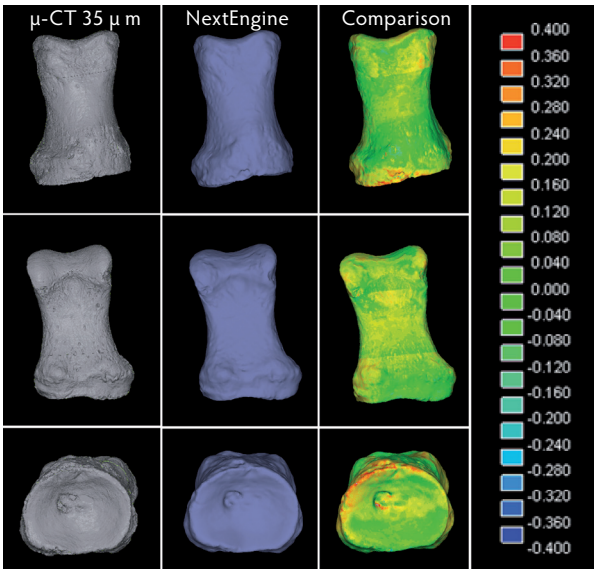

Fig. 13. Difference-map of µ-CT/NextEngine for Spy425. Generated by Steinbichler INSPECTplus with -0.4/0.4 mm scale.

Abb. 13. *Abweichungskartierung vom µCT/NextEngine für Spy 425. Erzeugt mit Steinbichler INSPECTplus mit einer -0,4/0,4 mm Skala.*

	COMET Inspect
CT - NEXTENGINE	
Average deviation	145 µm
Maximum deviation	731 µm

Fig. 14. Nominal-actual model of Spy18 obtained with COMET Inspect.

Abb. 14. *Soll-Ist Modell von Spy18, erzeugt mit dem Programm COMET Inspect.*

which can be used for isolated teeth, but this option is more difficult in the case of a complete skull or a large collection.

The comparative analysis of difference-mapping yields similar, though not identical results for the two softwares used in this study. Given that registration is fully automatic, it can be suggested that the difference in maximum deviation lies in details of the computational algorithms used in the two programs. However, these are not documented in detail, so that we are currently unable to demonstrate that this is indeed the case. Further analyses and, possibly, feedback from the software editors, are therefore required to address this issue appropriately.

The results of this comparative study demonstrate that the Breuckmann system consistently yields more reliable data, as measured by the standard deviation, than either the NextEngine or the COMET systems. Given the numerous technical differences between Breuckmann on the one hand and COMET / NextEngine on the other, it is impossible to identify which factor is responsible for this. Clearly, the combination of 2 cameras (versus 1), structured light (versus laser) and the reliance on two additional triangulation techniques (greycode and phase shift) all make a contribution.

In the case of small and medium size bones, the NextEngine scanner provides surface scans with a good level of details and accuracy and can easily

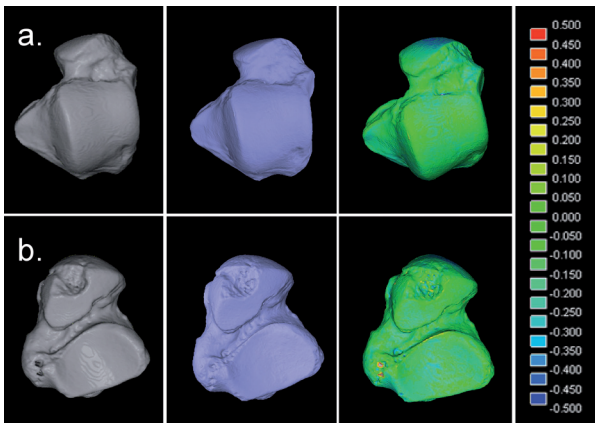

Fig. 15. Difference-map of medical CT/NextEngine for Spy 18. Generated by Steinbichler INSPECTplus with -0.5/0.5 mm scale.

Abb. 15. *Abweichungskartierung vom medizinischen CT/NextEngine für Spy 18. Erzeugt mit Steinbichler INSPECTplus mit einer -0,5/0,5 mm Skala.*

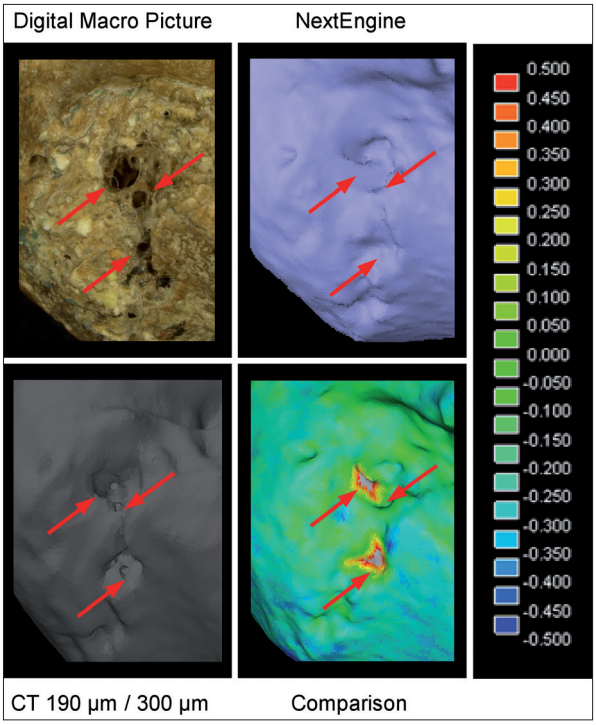

Fig. 16. Difference-map of medical CT/NextEngine for Spy18. Detailed view of cancellous bone area. Generated by Steinbichler INSPECTplus with -0.5/0.5 mm scale.

Abb. 16. *Abweichungskartierung vom medizinischen CT/NextEngine für Spy 18. Detailansicht des Bereichs mit freiliegender Spongiosa. Erzeugt mit Steinbichler INSPECTplus mit einer -0,5/0,5 mm Skala.*

replace the model produced from CT data, producing a higher quality of the external surface of the bone. Even though the ScanStudio application has improved a lot, it is possible that the use of an external application for post-treatment could provide still better 3D models. This is the option choosed by M. Tocheri, who uses the lower resolution and fast mode provided by the NextEngine scanner but increases the number of views to 16, which is the maximum allowed by the turntable system. Tocheri uses Scanstudio HD for scanning and finalizes the alignment of the views with Geomagic.

Acknowledgements: Special thanks go to STEINBICHLER and their members who helped us carry out tests with the COMET V. We would also like to thank Matthew W. Tocheri from the National Museum of Natural History, Smithsonian Institution (Washington DC) for tips concerning the settings of NextEngine and interesting discussions about the surface scanning of anthropological collections. MF was partially funded by NSF (SEI 05-13660).

Literature cited

Benazzi, S., Orlandi, M. & Gruppioni, G. (2009). Technical note: virtual reconstruction of a fragmentary clavicle. *American Journal of Physical Anthropology* 138(4): 507-514.

Borderie, Q., Torguet, P., Subsol, G., de Lumley, H., Mafart, B. & Jessel, J. P. (2004). *3D Modeling of Paleolithic Tools.* Workshop on Archaeology and Computers. Vienna, 3.-4. November 2004.

DeSilva, J. M. (2009). Functional morphology of the ankle and the likelihood of climbing in early hominins. *Proceedings of the National Academy of Sciences* 106 (16): 6567-6572.

Fraipont, J. & Lohest, M. (1887). La Race humaine de Néanderthal ou de Canstadt en Belgique. Recherches ethnologiques sur des ossements humains, découverts dans des dépôts quaternaires d'une grotte à Spy et détermination de leur âge géologique. *Archives de Biologie* 7 (1886): 587-757.

Gibbons, A. (2002). Glasnost for Hominids: Seeking Access to Fossils. *Science* 297: 1468-1468.

Guipert, G., Subsol, G., Jessel, J. P., Delingette, H. & Mafart, B. (2003). *The FOVEA Project: a New Look at Human Past.* 9th International Conference on Virtual Systems and Multimedia, Montreal (Canada), October 2003.

Kullmer, O., Huck, M., Engel, K., Schrenk, F. & Bromage, T. G. (2002). Hominid Tooth Pattern Database (HOTPAD) based on optical 3D topometry. *In:* B. Mafart & H. Delingette (Eds.) *Three–Dimensional Imaging in Paleoanthropology and Prehistoric Archaeology.* Acts of the XIVth UISPP Congress, University of Liège, Belgium, 2-8 September 2001, Colloque, Symposium 1.7 eds. , BAR International Series 1049: 71-82.

Mafart, B. & Delingette, H. (2002). *Three-Dimensional Imaging in Paleoanthropology and Prehistoric Archeology.* Archaeopress. British Archaeological Series 1049. Actes du XIVème Congrès UISPP.

Mafart, B., Guipert, G., de Lumley, M. A. & Subsol, G. (2004). Three-dimensional computer imaging of hominid fossils: a new step in human evolution studies. *Canadian Association of Radiologists Journal* 55/4: 264-270.

Recheis, W., Macchiarelli, R., Seidler, H., Weaver, D. S., Schaefer, K., Bondoli, L., Weber, G. W. & zur Nedden, D. (1999). New Methods and Techniques in Anthropology. *Collegium antropologicum* 23: 495-509

Rougier, H., Crevecoeur, I., Fiers, E., Hauzeur, A., Germonpré, M., Maureille, B. & Semal, P. (2004). Collections de la Grotte de Spy: (re)découvertes et inventaire anthropologique. *Notae Praehistoricae* 24: 181-190.

Schmitz, R. (2003). Interdisziplinäre Untersuchungen an den Neufunden aus dem Neandertal. *Mitteilungen der Gesellschaft für Urgeschichte* 12: 25-45.

Semal, P., Toussaint, M., Maureille, B., Rougier, H., Crevecoeur, I., Balzeau, A., Bouchneb, L., Louryan, S., Declerck, N. & Rausin, L. (2005). Numérisation des restes humains néandertaliens belges: préservation patrimoniale et exploitation scientifique. *Notae Praehistoricae* 25: 25-38.

Semal, P., Rougier, H., Crevecoeur, I., Jungels, C., Flas, D., Hauzeur, A., Bocherens, H., Cammaert, L., De Clerck, N., Germonpré, M., Hambucken, A., Higham, T., Maureille, B., Pirson, S., Toussaint, M. & van der Plicht, J. (2009). New Data on the Late Neandertals: Direct Dating of the Belgian Spy Fossils. *American Journal of Physical Anthropology* 138: 421-428.

Singleton, M. (2003). Functional and phylogenetic implications of molar flare variation in Miocene hominoids. *Journal of Human Evolution* 45 (1): 57-79.

Slizewski, A. & Semal, P. (2009). Experiences with low and high cost 3D surface scanner. *Quartär* 56: 131-138.

Sumner, T. A. & Riddle, A. (2008). A Virtual Paleolithic: Assays in Photogrammetric Three-Dimensional Modelling. *PaleoAnthropology* 2008: 158-169.

Tocheri, M. W., Orr, C. M., Larson, S. G., Sutikna T., Jatmiko Saptomo E. W., Awe Due, R., Djubiantono, T., Morwood, M. J. & Jungers, W. L. (2007). The Primitive Wrist of Homo floresiensis and Its Implications for Hominin Evolution. *Science* 317 (5845): 1743-1745.

Ulhaas, L., Kullmer, O. & Schrenk, F. (2007). Tooth wear diversity in early hominid molars – a case study. *In:* S. Bailey & J.-J. Hublin (Eds.) *Dental Perspectives on Human Evolution: State of the Art Research in Dental Anthropology.* Springer.

Weber, G. W., Recheis, W., Scholze, T. & Seidler, H. (1998). Virtual Anthropology (VA): Methodological Aspects of Linear and Volume Measurements - First Results. *Collegium antropologicum* 22: 575-584.

Weniger, G.-C., Döllner, J., Macchiarelli, R., Mandel, M., Mayer, P., Radovcic, J. & Semal, P. (2007). The Neanderthal TOOLS and NESPOS. *In:* A. Figueiredo & G. Leite Velho (Eds.) *The World is in your eyes.* Computer Applications in Archaeology Conference 2005, Tomar, 267-269.